NUKLEONIKA 2013;58(2):333–338

ORIGINAL PAPER

Algorithms for digital γ-ray spectroscopy

Zbigniew Guzik,
Tomasz Krakowski

Abstract. The data processing in modern nuclear spectroscopy is dominated by digital methods. In this paper we present a full set of algorithms necessary for energy reconstruction, baseline restoration, trigger generation and selection of events (acceptation) which are based on digital signal processing (DSP) techniques. All algorithms were fully evaluated using mathematical apparatus of Z-transform. The energy reconstruction algorithm is based on trapezoidal shaping. The baseline restoration makes the use of a digital moving average, while trigger generation algorithm utilize a digital form of RC-CR2 filter with protection windowing. The evaluated algorithms has been implemented and used in the demonstrator build for national borders protection.

Key words: data acquisition • digital spectrometry • digital signal processing (DSP) • gamma spectroscopy • Z-transform

Z. Guzik✉, T. Krakowski
National Centre for Nuclear Research (NCBJ),
7 Andrzeja Sołtana Str., 05-400 Otwock/Świerk, Poland,
Tel.: +48 22 718 0549, Fax: +48 22 779 3481,
E-mail: zbigniew.guzik@ncbj.gov.pl

Received: 7 November 2012
Accepted: 8 May 2013

Introduction

The task of electronics in nuclear physics detection systems is to collect the electrical charge deposited in a radiation detector and to convert it into a digital code to be further analyzed by a main computer. In most cases the quantities of interest are the particle energy and the time of particle occurrence. The traditional spectroscopy system for the particle detectors [2] have been made of almost all analog parts constituting a chain of preamplifier, shaping amplifier and peak sensing analog-to-digital converter (ADC) configured as separate units. Introduced recently a digital approach to nuclear spectroscopy greatly simplifies the apparatus and has the following advantages:

– repeatability and programmability,
– time and temperature stability,
– lower cost,
– reduction of dead time and ballistic deficit elimination,
– lack of expensive spectrometric amplifier,
– simplicity in tuning and debugging.

The goal of our investigation was to build a demonstrator of a national border protection system that would scan passing large-dimension cargo (e.g. trucks, containers) with beams of ionizing radiation in order to detect illegal trafficking of various prohibited substances by means of an innovative combination of radiography and activation techniques.

For the purpose of this project, we developed a set of algorithms to be used in the digital spectrometric

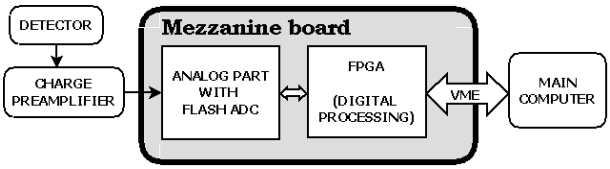

Fig. 1. Block diagram of the DSP spectrometric channel.

channel containing all necessary data acquisition elements (hybrid charge preamplifier was also included). All DSP calculations were performed by field programmable gate array (FPGA) and obtained results (values of deposited energy) accompanied by a time stamp were sent directly to the main computer via VME bus.

The simplified block diagram of digital spectrometric channel is shown in Fig. 1. As can be seen, it is much simpler than the analog solution. Almost entire electronics is located on a small mezzanine board. Evaluated algorithms were focused on energy reconstruction, baseline restoration, trigger generation and event acceptance. All algorithms derivation and description were conducted fully with the application of Z-transform.

In mathematics and signal processing, the Z-transform converts a time-domain signal, which is a sequence of real or complex numbers, into a complex frequency--domain representation. Each typical time-domain signal has its equivalent in Z-transform domain.

Energy reconstruction

The key concept in digital γ-ray spectrometry is the algorithm of filtering the incoming sampled data from the preamplifier into a form suitable for precise determination of accumulated energy. In the field of digital spectrometry three such algorithms can be distinguished: Gaussian algorithm [6], "cusp" algorithm [5] and trapezoidal algorithm [1, 3, 4]. The most optimal and widely used one is the trapezoidal algorithm, which was chosen for our needs. Known trapezoidal shaping algorithms were evaluated with the help of complicated time domain equations. We propose another approach based on Z-transform evaluation.

The general convolution leading to the trapezoid is as follows

$$F_{TPZ}(z) = F_{IN}(z) * H_{SHA}(z) \tag{1}$$

From where the expected shaping transmittance (transfer function) has the form

$$H_{SHA}(z) = \frac{F_{TPZ}(z)}{F_{IN}(z)} \tag{2}$$

where $F_{TPZ}(z)$ is the transfer function of the trapezoid itself and $F_{IN}(z)$ is the transfer function of the input wave from the preamplifier.

Characteristics of the signal from a preamplifier

Any radiation event produces in the detector an amount of charge $q(t)$ proportional to the absorbed energy E, so the signal from a spectrometric charge preamplifier is a convolution of this charge signal and preamplifier impulse response $h(t)$

$$f(t) = \int_{-\infty}^{+\infty} q(t') * h(t - t')dt' \tag{3}$$

The charge distribution function from the detector is characterized by a very short leading edge in the range of single nanosecond and the falling edge which depends on the type of used scintillator – usually this time, expressed by the approximated time constant F, is in the range of tenth of nanoseconds up to microsecond. The charge signal from the detector is as follows

$$q(t) = E\, e^{-\frac{t}{F}} \tag{4}$$

Preamplifier impulse response function is shown below

$$f_{RC}(t) = \begin{cases} \exp(-t/T) & \text{for } t \geq 0 \\ 0 & \text{for } t < 0 \end{cases} \tag{5}$$

where T is the time discharge constant, which usually is in the range of tenth of microseconds. The final equation for signal from the preamplifier is

$$f(t) = E\left(e^{-\frac{t}{T}} - e^{-\frac{t}{F}}\right) \tag{6}$$

The time constants T and F differs up to in three orders of magnitude, so the constituent in Eq. (6), concerning the detector time constant can be ignored – it is assumed that energy impulse from the detector has the form of $\delta * E$, where δ is the Dirac delta and E is the value of the accumulated energy. Equation for $F_{IN}(z)$ transmittance from Eq. (2) has, in Z-transform domain, the following form

$$f(t) = E\, e^{-\frac{t}{T}} \Rightarrow F_{IN}(z) = E\frac{z}{z-\beta} = E\frac{1}{1-\beta z^{-1}} \tag{7}$$

Factor β is a pole-zero cancellation coefficient of exponential shape and has the form

$$\beta = e^{-\Delta t/T} \tag{8}$$

where Δt is the sampling period. Time constant F is ignored in trapezoidal shaping, however it is important in algorithm of trigger generation.

Synthesis of the trapezoid wave

As seen in Fig. 2, a trapezoid wave may by synthesized by the sum of four items

$$f_{TPZ}(t) = f_A(t) + f_B(t) + f_C(t) + f_D(t) \tag{9}$$

Linear pulse $f_A(t)$ may be expressed in the time domain and Z-transform domain as

$$f_A(t) = \frac{E}{t_1}t \Rightarrow F_A(z) = \frac{E}{R}\frac{z}{(z-1)^2} \tag{10}$$

Assuming symmetrical shape of the trapezoid, the following time assignments were given;

$$t_1 = R\Delta t, \quad t_2 = (R+M)\Delta t, \quad t_3 = (R+M+R)\Delta t \tag{11}$$

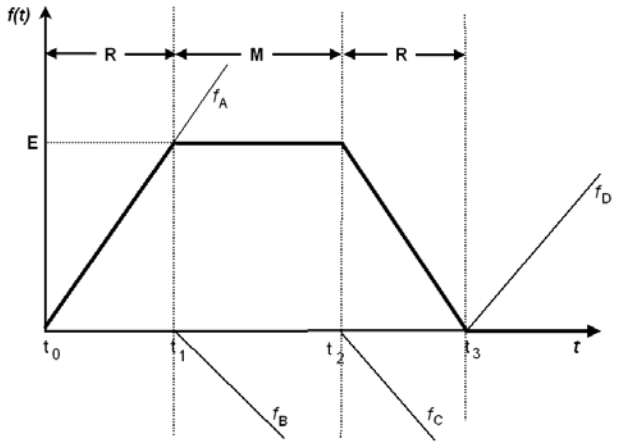

Fig. 2. Synthesis of the trapezoid.

where R are the trapezoid edges and M is the trapezoid top. Remaining three linear pulses can be expressed by means of a delayed $FA(z)$ function with adequate polarities

$$\begin{aligned} F_B(z) &= -F_A(z) * z^{-R} \\ F_C(z) &= -F_A(z) * z^{-(R+M)} \\ F_D(z) &= +F_A(z) * z^{-(R+M+R)} \end{aligned} \tag{12}$$

The sum of all linear pulse components has the following form in Z-transform domain

$$F_{TPZ}(z) = \frac{E}{R}(1 - z^{-R} - z^{-(R+M)} + z^{-(R+M+R)})\frac{z}{(z-1)^2} \tag{13}$$

which can be converted into the final trapezoid transmittance:

$$F_{TPZ}(z) = \frac{E}{R}(1 - z^{-R})(1 - z^{-(R+M)})\frac{z^{-1}}{(1 - z^{-1})^2} \tag{14}$$

Final trapezoidal shaping algorithm

From Eqs. (2), (7) and (14) the following expression (convolution) can be obtained

$$F_{TPZ}(z) = (1 - z^{-R}) * (1 - z^{-(R+M)}) * \frac{(1 - \beta z^{-1})}{1 - z^{-1}} * \frac{z^{-1}}{1 - z^{-1}} * \phi \tag{15}$$

This is the final form of the algorithm for energy determination, where ϕ is the normalization coefficient ($1/R$) and β is the pole zero cancellation factor expressed by Eq. (8). Presented expression, being a combination of FIR and IIR filters, describes linear time invariant (LTI) system. It means that realization of the shaping circuit can be subdivided into independent operations executed in any order. However, to achieve maximal precision, it is recommended to follow the order shown in Eq. (15). The graphical representation of developed algorithm is presented in Fig. 3. The Z^{-N} node is the digital delay for N cycles.

In order to improve energy resolution it is recommended to provide an additional averaging of the top,

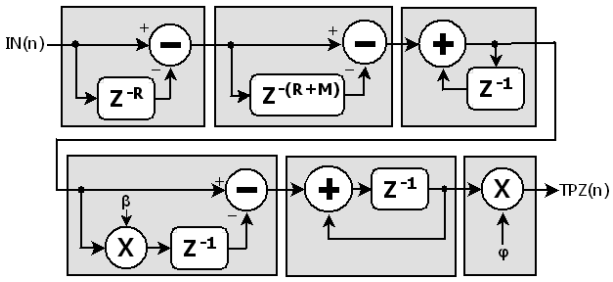

Fig. 3. Graphical representation of trapezoidal shaping algorithm.

flat part of the trapezoid. This procedure, performed by a moving average node, will reduce high frequency noises, which remain after initial averaging. Length of the averaging window is expressed by an A parameter. Figure 4 shows trapezoidal shape with basic conversion parameters where some of them are related to the baseline restoration.

Baseline restoration

The output of an analog pulse preamplifier typically shows some amount of bias caused by the detector leakage current, electronic circuitry and so on. Additionally, due to noise pickup or variations in the detector leakage current, the baseline shows continuous time drift. Trapezoid shaping does not eliminate this baseline, so it should be found and subtracted from the raw trapezoid wave. Baseline determination is realized by digital averaging of the trapezoid wave in cases when spectrometric channel is not busy and actual trapezoid amplitude is inside a window represented by B parameter (Fig. 4).

The averaging is performed by moving average node of the Q window value. Trigger generation algorithm is characterized by a certain amount of latency, so in order to exactly synchronize trapezoid with the trigger pulse, it is necessary to delay the trapezoid wave – the trigger should minimally precede the starting point of the first trapezoid edge. The resulting baseline value is latched in the moment of trigger occurrence.

Trapezoidal shaping algorithm has a continuous accumulation element which remembers all "history" of processed waves starting from the time of initialization. Due to the irregularity of input wave, caused mainly by signal over-range, this accumulation element may collect unwanted redundancy data. So, if value trapezoid bottom line or calculated baseline exceeds (in both sides) the B value, the mentioned accumulation element will be zeroed.

Trigger generation

The trigger pulse is the main reference for all DSP calculation – its quality is of primary importance and has a dominating influence on the energy resolution of conducted measurements. Good trigger should be characterized by a low detection level, high noise immunity, a low dead time and a very low dispersion. Our trigger generation algorithm consists of the two following distinct phases.

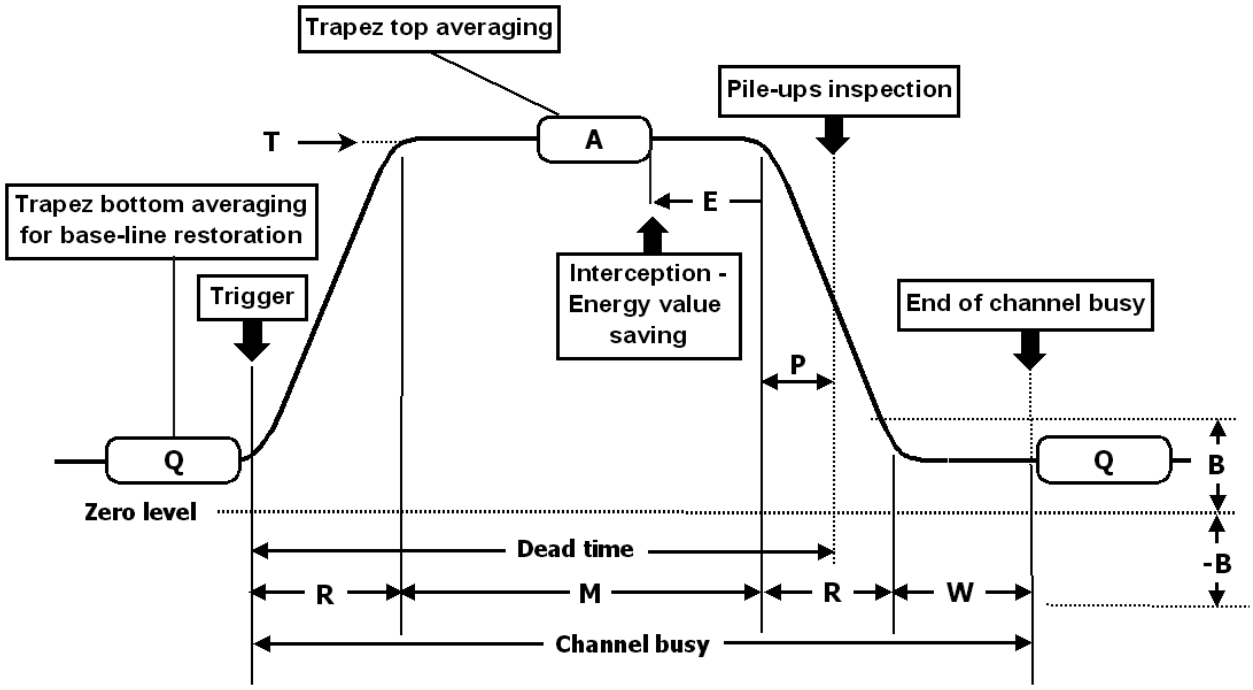

Fig. 4. Basic parameters for the energy reconstruction.

Timing filter phase

The responsibility of timing filter phase is to convert the input wave into a form suitable for extraction of precise, well determined time reference of incoming discrete pulse. The result of this phase, performed by a timing filter, is smoothed bipolar pulse. Representation of the timing filter in Z-transform domain, called also RC-CR2 filter, is as follows

$$H_{TF}(z) = \frac{z^{-1}(1-z^{-C})}{1-z^{-1}} * (1-z^{-F}) * (1-z^{-F}) \tag{16}$$

and is composed of three elements:

- **Smoothing.** This procedure (moving average) is indispensable, because high frequency noises in the input signal may cause false triggers and instability of the front edge detection. The time window in moving average is controlled by C parameter.
- **First differentiation** removes from the input wave all low frequency components, i.e. baseline and discharge exponent. This procedure is realized by digital differentiation node where time of differentiation (parameter F) is usually equivalent to the leading edge of the signal from the preamplifier.
- **Second differentiation** produces a bipolar wave, whose zero crossing point is independent of the input signal amplitude (like in Constant Fraction Discrimination). Differentiation constant (parameter F) is the same as in the first differentiation.

Zero crossing detection phase

Zero crossing detection operation is rather straightforward, but in our case it should be supported with an isolation mechanism, which can distinguish proper one from many other false trigger occurrences caused mainly by noise. This phase is composed of the following operations:

- **Leading edge recognition – sense window.** In the moment, when value of the signal from timing filter exceeds a certain threshold level J, the sense window is started – the length of this window is equal to twice of F parameter. Because of the noises, the leading edge detection should be verified – the edge detection is assumed valid, when the value of signal from the timing filter is above the threshold during Y consecutive cycles – this can be understand as some kind of hysteresis.
- **Trigger generation.** Detection of zero crossing (generation of trigger pulse) occurs when the signal from the timing filter crosses zero level. The effective trigger is generated only, when the signal from zero crossing detectors occurs during the time duration of sense window.
- **Veto window.** At the moment of trigger generation, the second, veto window of time V is started. During course of this window all further triggers are inhibited. This prevents appearance of the false triggers originating in the timing filter and leading edge detector.

Figure 5 shows the signals flow chart during execution of the trigger generation algorithm.

Event acceptation

There exist three important time reference points having a crucial impact on the quality of the measurement (Fig. 4). First reference is the "interception" point, which is the time when the calculated energy value is temporarily saved. This time is established backward to the end of trapezoid top and is described by $\{R + M - E\}$. The optimal value of E parameter is $1/8*M$.

The second important reference is the point where pile-ups are inspected. This point, expressed by $\{R + M$

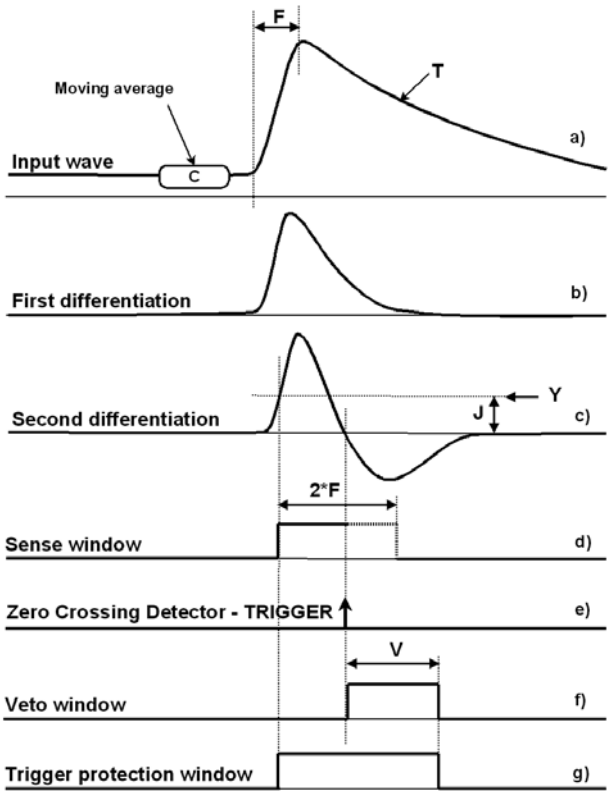

Fig. 5. Timing diagrams of trigger generation procedures.

$+ P\}$, is located after the top of the trapezoid; however recommended value of E parameter is zero. And the third, last reference is the time which establishes time zone when the spectrometric channel is busy. This time, used for baseline reconstruction disabling, is given by $\{R + M + R + B\}$.

The event is considered valid when the three following conditions are fulfilled:

- **External gating condition** – in the moment of trigger generation external gating signal should be high in coincidence mode or low in veto mode (this condition is optional and may be omitted).
- **Energy condition** – in the moment of interception the calculated energy value should be higher than the preset energy low threshold and lower than the energy high threshold**.**
- **Lack of pile-ups condition** – up to the point of pile-up inspection no pile-up or input signal over-range is detected.

If any of the above condition is not met, the event will be rejected. Valid event data are transferred to the main computer and may also be used to create local histograms.

Results

All the developed and described above algorithms were implemented in hardware (instantiated in FPGAs) and successfully used in the AiD project ("Development of dedicated systems based on accelerators and detectors of ionizing radiation for medical therapy and in the detection of hazardous materials and toxic wastes"). The four spectroscopy channels were incorporated into the VME data acquisition board accompanied with four tag channels, based on constant fraction discrimination, for time measurements. The sampling Flash ADC rate was set to 50 MHz and the 32-bits basic calculation accuracy was chosen.

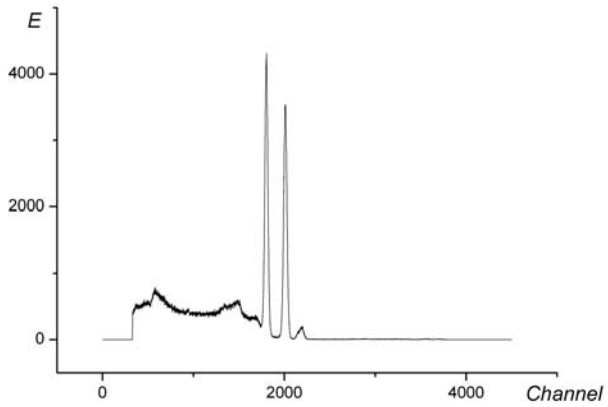

Fig. 6. The spectrum of ^{60}Co measured with $LaBr_3$.

The VME acquisition board has been designed and is used in the prototype device for isotope analysis and identification of concealed or otherwise inaccessible materials. At the moment, it processes signals from two spectroscopic gamma detectors and one neutron counter. The two gamma detectors work in the anti-coincidence mode, so apart from the amplitude processing and/or signal registration, the time of an event arrival has to be recorded.

Figure 6 shows the gamma spectrum of ^{60}Co radiation source that was measured with a $LaBr_3$ scintillator using a PMT readout, a Cremat CR-113 charge sensitive preamplifier and our DSP analyzer. The energy resolution of 2.07 ± 0.04% and 2.01 ± 0.04% was obtained for the 1173.2 and 1332.5 keV full energy peaks, respectively. The source of the third peak on the right is self-activity of lanthanum [7] in the $LaBr_3$ scintillator which was chosen for our setup. The low energies were discarded up to the channel 30 by an event acceptation criterion. Note the excellent performance of the gamma spectrometer.

Acknowledgment. The authors wish to thank Prof. M. Moszyński for stimulating discussions. The results presented in this paper have been obtained within the project "Development of dedicated systems based on accelerators and detectors of ionizing radiation for medical therapy and in detection of hazardous materials and toxic wastes" of the EU Structural Funds (Project no. POIG.01.01.02-14-012/08-00).

References

1. Georgiev A, Gast W (1993) Digital pulse processing in high resolution high throughput gamma-ray spectroscopy. IEEE Trans Nucl Sci 40;4:770–779
2. Guzik Z, Borsuk S, Traczyk K *et al*. (2006) TUKAN-an 8K pulse height analyzer and multichannel scaler with a PCI or a USB interface. IEEE Trans Nucl Sci 53;1:231–235
3. Imperiale C, Imperiale A (2001) On nuclear spectroscopy pulses digital shaping and processing. Measurement 30:49–73

4. Jordanov VT, Knoll GF (1994) Digital synthesis of pulse shapes in real time in high resolution radiation spectroscopy. Nucl Instrum Methods A 345:337–345
5. Jordanov VT, Knoll GF, Huber AC, Pantazis JA (1994) Digital techniques for real-time pulse shaping in radiation measurements. Nucl Instrum Methods A 353:261–264
6. Kihm T, Bobrakov VF, Klapdor-Kleingrothaus HV (2003) A digital multichannel spectroscopy system with 100 MHz flash ADC module for the GENIUS-TF and GENIUS projects. Nucl Instrum Methods A 498:334–339
7. Nicolini R, Camera F, Blasi N *et al*. (2007) Investigation of the properties of a 1"x 1" LaBr3:Ce scintillator. Nucl Instrum Methods A 582:554–561